JOURNAL OF SOLID STATE CHEMISTRY **15**, 352–359 (1975)

On the Structure of Evaporated Bismuth Oxide Thin Films*

JOHN W. MEDERNACH†

College of Ceramics, Alfred University, Alfred, New York 14802

Received March 27, 1974; in revised form April 8, 1975

The bismuth oxide films evaporated from bulk Bi_2O_3 are shown to vary in stoichiometry. The as-evaporated low rate (1–5 Å/sec) films are microcrystalline and bismuth rich, relative to Bi_2O_3, and their optical absorption edge broadens and shifts to lower energies. High rate (15–25 Å/sec) films are morphous and oxygen-rich with an absorption edge shifted to higher energies. Thermal decomposition of the Bi_2O_3 during evaporation produces the variations in film stoichiometry. The high temperature δ-Bi_2O_3 observed in the as-evaporated low rate films and thermally treated amorphous films indicates the melt and the films are structurally similar. Thermal treatment of the low rate films results in the formation of the β-form. Comparison of X-ray and stoichiometry results suggests that β-Bi_2O_3 be expressed as β-$Bi_2O_{\pm 3x}$, where x is the deviation from trioxide stoichiometry.

Introduction

Numerous studies (*1–19*) have been reported concerning the characterization and identification of phases present in the bismuth–oxygen system. However, disagreement still exists regarding the identity and the stoichiometry of the phases present in samples prepared by various techniques (*1–5*, *8*, *10–15*). Bismuth trioxide possesses a number of different polymorphs. The monoclinic α-form is the stable low temperature form. The tetragonal β-form is metastable and can be obtained by quenching (*4*) or by decomposition (*14*). The high temperature δ-form (*1*, *2*) is a cubic phase which exists between 740 and 825°C. The metastable γ-form is a body-centered cubic phase which is formed by controlled cooling of the β-form. Some investigators (*2*) also have proposed the designation δ^*, β^*, and γ^* for the impurity forms of the cubic, tetragonal, and b.c.c. Bi_2O_3 phases, respectively. A new space group $P\bar{4}2_1c$ is proposed for both β-Bi_2O_3 (*16*) and nonstoichiometric β-$Bi_2O_{2.5}$ (*5*) as a result of recent studies. A suboxide BiO (*17*, *18*) observed during the early stages of oxidation of bismuth also is reported to be unstable (*19*). The structural information available for these phases are summarized in Table I along with other bismuth oxide phases.

Nonstoichiometric oxide films formed by evaporation of a metal oxide occur because of the incongruent evaporation of the oxide. Studies (*20*) show that a large number of oxides dissociate at high temperatures, and this is also suggested for Bi_2O_3 (*21*). Higher oxides such as Bi_2O_3 tend to lose oxygen at elevated temperatures which is observed during the evaporation of Bi_2O_3 (*22*, *23*). It was suggested in a recent publication (*24*) that the stoichiometry of evaporated bismuth oxide films can be determined by relating the bismuth content of the sample film to the broadening of its optical absorption edge. This study was initiated to determine the effect of the variation in the

---

* A table of *d*-values and other supporting material has been deposited as Document No. NAPS-02582 with the ASIS National Auxiliary Publications Service, c/o Microfiche Publicat., 440 Park Avenue South, New York, New York 10016. A copy may be secured by citing the document number and by remitting $5.00 for photocopies or $1.50 for microfiche. Advance payment is required. Make check or money order payable to Microfiche Publications.

† This paper is based on work submitted in partial fulfillment of the requirements for the Ph.D. degree, Alfred University, Alfred, N.Y. 1973.

TABLE I

BASIC STRUCTURAL INFORMATION FOR THE BISMUTH OXIDES

Compound	System	a (Å)	b (Å)	c (Å)	Ref.
α-Bi_2O_3	Monoclinic $P2_1/c$	5.83	8.14	7.48[a]	(*1*, *11*)
	Pseudoorthorhombic	5.85	8.16	13.83	(*13*, *14*)
α-Bi_2O_3	Monoclinic $P2_1/c$	5.848	8.166	7.510[b]	(*12*)
β-Bi_2O_3	Tetragonal $C\bar{4}2b$	10.95	—	5.63	(*4*)
		10.93	—	5.62	(*1*)
β-Bi_2O_3	Tetragonal $P\bar{4}2_1c$	7.7425	—	5.6313	(*16*)
δ-Bi_2O_3	Cubic $Fm3m$	5.66	—	—	(2)
δ-Bi_2O_3	Cubic $Pm3m$	5.525	—	—	(*1*)
γ-Bi_2O_3	Cubic	10.25	—	—	(*15*)
γ-Bi_2O_3	Cubic $I23$	10.24	—	—	(*1*)
β-$Bi_2O_{2.5}$	Tetragonal $P\bar{4}2_1c$	7.75[c]	—	5.63	(5)
$Bi_2O_{2.35}$	Tetragonal $I4/mmm$	3.85[c]	—	35.1	(7)
$Bi_2O_{2.75}$	Tetragonal $I4/mmm$	3.85[c]	—	12.25	(6)
BiO	Hexagonal $-R3m$	3.88[c]	—	9.71	(*17*)
BiO	Cubic (NaCl)	5.69[c]	—	—	(*18*)

[a] $\beta = 112.53°$.
[b] $\beta = 113.0°$.
[c] Based on electron diffraction results.

stoichiometry of bismuth oxide thin films upon their structure. Both the deviations in the films' stoichiometry and other phases present are discussed with respect to their evaporation rates and thermal treatments.

Experimental

All evaporations were made in a vacuum system capable of achieving a minimum pressure of less than 5×10^{-7} torr. Bismuth trioxide, 99.999% pure, obtained from Alpha Inorganics was evaporated from a platinum boat. The evaporation rate was varied from 1 to 25 Å/sec. The thickness was monitored during deposition and several samples also were checked independently using the Tolansky technique. MgO single crystal 1 × 1 cm and glass 2.5 × 2.5 cm substrates were employed. The film thickness was varied from 2000 Å to 5000 Å. The substrate cleaning is described elsewhere (*22*).

Because of possible reactions between the Bi_2O_3 and the platinum boat, several films and samples of the residue in the platinum boat were analyzed for platinum content using atomic absorption spectroscopy. The platinum contamination never exceeded 0.029 wt% and no correlations were observed with the evaporation rate, the structural or optical properties.

The thermal treatment employed in this investigation was similar to that of Halford and Hacker (*25*). These films evaporated between 1 and 5 Å/sec were treated in oxygen (1 torr) at 150°C for periods between 15 and 180 min. To determine the effect of oxygen on the structural properties, several films were treated in air or vacuum (10^{-2} torr) at 150°C.

Two sets of films evaporated consecutively at 25 Å/sec were prepared for the stoichiometry determination. The bismuth–oxygen ratio was determined by electron probe analysis for a set of films having a thickness of 1.5 μm. The second set, which possessed a thickness of 0.3 μm was used in the optical measurements to determine the absorption coefficient. The photon energy values for these samples for an absorption coefficient of 1.6×10^5 cm^{-1} yielded a linear plot with respect to the Bi/O ratio. This method was used to determine the compositions of the as-evaporated and thermally treated films. The transmittance T and the reflectance R were measured with a Beckman DK-2A Ratio Recording Spectrophotometer. The absorption coefficient α was calculated from the expression $T \approx (1 - R)^2 \exp(-\alpha d)$, where d is the film thickness.

X-ray diffraction profiles were made on all samples using a Norelco diffractometer with a graphite crystal monochromator. Diffraction profiles were run from 20–80° (2θ) using copper K_α radiation. The lattice parameters were determined with a 114.59 mm diameter Debye–Scherrer powder camera, and gold over the bismuth oxide was used to calibrate. The experimental d-values were indexed using a calculated powder pattern as well as a computer indexing program (*26*). The front and back reflection d-values were obtained by oscillating the film sample through an angle of 120 (±60°) at 2 Hz. The air–film interface was mounted at the centerline of the camera axis normal to the beam. A General Radio 1750-A Sweep Drive was employed to oscillate the samples. The reflections from 165–180° (2θ) were not observed due to the position of the collimator. Asymmetric line broadening due to the oscillation of the sample was not detected. Exposure time varied from 10–22 hr for MgO and glass substrates, respectively.

Calculated X-ray powder patterns were made for all reported forms of bismuth oxide. These calculated patterns included corrections for anomalous dispersion using Cromer polynomial form factors Bi^{3+} and O^{2-}. The lattice parameters were refined using a least-square procedure (*26*). This procedure did not yield any error statistics with the refined lattice parameters, so a number of measurements were made on each sample in order to obtain the standard deviations.

Additional films 320 Å thick were prepared on carbon coated grids and freshly cleaved NaCl crystals for the electron microscope. Some films also received the above mentioned thermal treatment. RCA EMU-3 and Hitachi electron microscopes were employed.

Results and Discussion

Microcrystalline and amorphous bismuth oxide films are observed at low and high evaporation rates, respectively. All as-evaporated bismuth oxide films produced almost identical amorphous X-ray diffraction patterns, showing a single broad peak at 28° (2θ). Low rate films (1–5 Å/sec) prepared for the electron microscope produced both electron diffraction ring and spot patterns, suggesting that the low-rate films are microcrystalline. The orientation observed most frequently is illustrated in Fig. 1, and identified as δ-Bi_2O_3 with a [111] zone axis, and patterns with a [001] orientation were observed. The disregistry of the spots in Fig. 1 is caused by a number of single crystallites in nearly perfect alignment. The calculated d-values agreed with the values for Sillén's (*1*) primitive cell rather than those for the f.c.c. cell proposed by later investigators (*2*). Amorphous bismuth

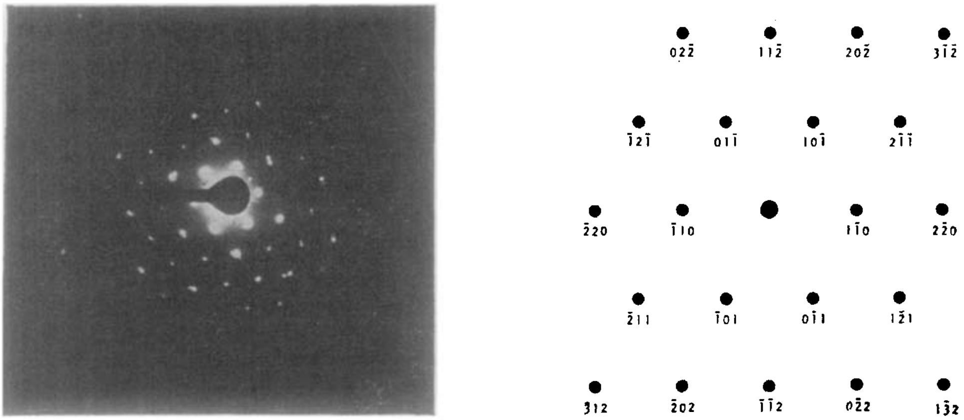

FIG. 1. Spot patterns of δ-Bi_2O_3 observed with low-rate films, [111] zone axis.

oxide films are formed at high rates (15–25 Å/sec) of deposition (*22*, *23*). Extremely fine crystallites on the order of 20–30 Å and possible structural defects in the amorphous films produced diffuse halo electron diffraction patterns. The microcrystalline or amorphous films can be crystallized by heating the samples in the electron beam, or by heating thicker samples in air or oxygen. Heating the film samples in the electron beam resulted in ring patterns identified as δ-Bi_2O_3, this pattern is illustrated in Fig. 2. The specimen temperature was not controlled in this study, but in another investigation (*23*) temperature control was employed, identical results are reported. Temperatures of 250–300°C are necessary to crystallize an amorphous film in contrast to the 150°C required for the microcrystalline films. A lattice parameter of $a = 5.52 \pm 0.02$ Å was calculated from electron diffraction measurements, and this value agrees with the lattice parameter obtained by several investigators (*4*, *9*, *14*, *23*). The formation of δ-Bi_2O_3 from an amorphous film as well as the formation of the film by evaporation indicates that the film and the Bi_2O_3 melt are structurally similar. This behavior also was observed for glassy $ZnCl_2$ (*27*).

All low rate as-evaporated films are devitrified by thermal treatment in oxygen. Both the 320 Å and the thicker films on glass substrates can be indexed on the basis of using the Gobel–Wilson indexing scheme (*26*), showing the observed and calculated values of $\sin^2_\theta$, agreed within 0.53%. The experimental X-ray d-values are compared with the calculated d-values for β-Bi_2O_3 and β-$Bi_2O_{2.5}$ in Table II. Thicker films (5000 Å) are used

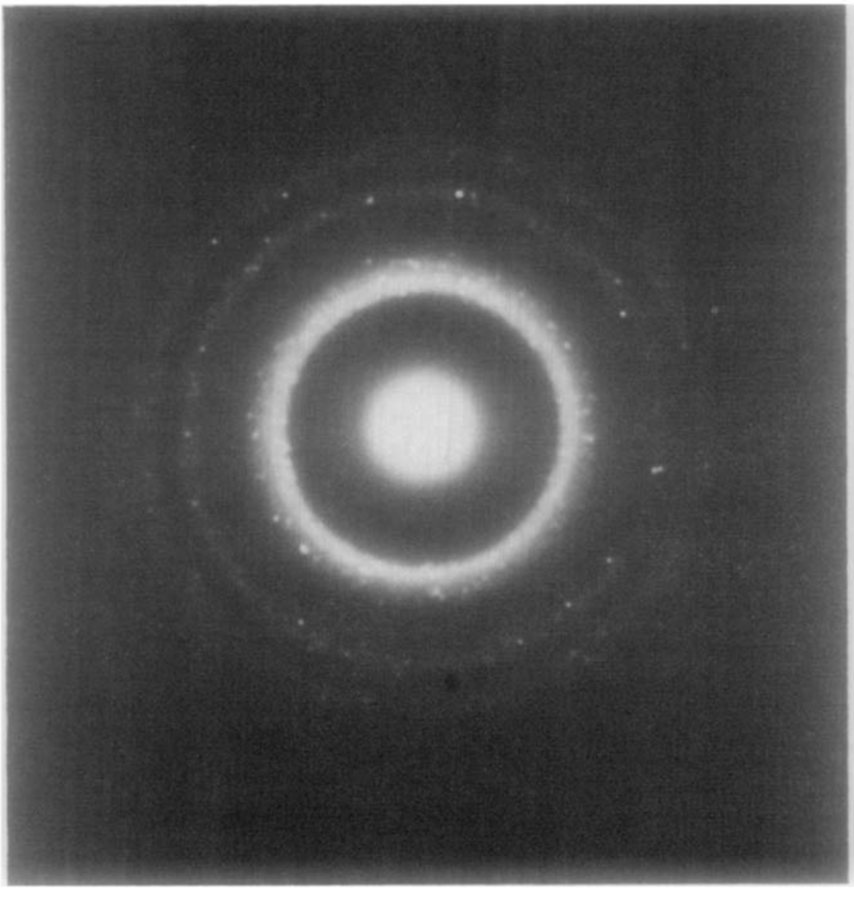

FIG. 2. δ-Bi_2O_3 ring pattern.

TABLE II

CALCULATED AND OBSERVED *d*-VALUES FOR THERMALLY TREATED BISMUTH OXIDE FILMS.[a]

Observed						Calculated										
Powder[b]		Glass[c]		[100] MgO[c]		β-Bi_2O_3[d]					β-$Bi_2O_{2.5}$[e]					
d(Å)	I/I_o	d(Å)	I/I_o	d(Å)	I/I_o	d(Å)	h	k	l	I/I_o	d(Å)	h	k	l	I/I_o
						5.474	1	1	0	2					
3.450	6					3.462	2	1	0	3	3.466	2	1	0	1
3.182	100	3.189	100	3.195	100	3.190	2	0	1	100	3.190	2	0	1	100
2.937	2					2.949	2	1	1	2	2.951	2	1	1	3
2.812	17	2.828	14	2.828	17	2.815	0	0	2	15	2.815	0	0	2	16
2.732	28	2.728	28	2.740	26	2.737	2	2	0	25	2.740	2	2	0	26
						2.646	1	0	2	1					
		2.495	2								2.504	1	1	2	1
		2.454	2								2.451	3	1	0	1
2.354	3					2.346	3	0	1	1					
2.175	2	2.184	3			2.184	2	1	2	1	2.185	2	1	2	1
2.149	1	2.149	3			2.147	3	2	0	1	2.149	3	2	0	1
2.004	1					2.006	3	2	1	1	2.008	3	2	1	1
1.959	25	1.963	18	1.967	20	1.963	2	2	2	22	1.964	2	2	2	23
1.931	13	1.927	8	1.935	7	1.936	4	0	0	11	1.937	4	0	0	10
1.865	2					1.878	4	1	0	1	1.879	4	1	0	2
1.776	2					1.781	4	1	1	2	1.783	4	1	1	2
											1.708	3	2	2	1
1.687	9	1.693	8	1.699	11	1.689	2	0	3	11	1.689	2	0	3	12
1.654[f]	19	1.651[f]	14	1.654[f]	17	1.655	4	2	1	20	1.656	4	2	1	19
						1.650	2	1	3	12					
1.591	9	1.593	6	1.595	7	1.595	4	0	2	8	1.596	4	0	2	8
						1.562	4	1	2	1	1.563	4	1	2	1
						1.548	4	3	0	1	1.550	4	3	0	1
1.485	1			1.491	1	1.493	4	3	1	1	1.494	4	3	1	1
1.403	2			1.414	1	1.408	0	0	4	2	1.407	0	0	4	1
1.368	4	1.365	3	1.368	2	1.368	4	4	0	2	1.370	4	4	0	2
						1.357	4	3	2	1					
1.325	1					1.328	4	1	3	1	1.328	4	1	3	1
1.273	8	1.272	5	1.275	5	1.273	6	1	0	6	1.274	6	1	0	6
1.254	3	1.255	5	1.256	4	1.258	6	0	1	3	1.259	6	0	1	2
						1.252	2	2	4	3	1.252	2	2	4	3
						1.242	6	1	1	1	1.247	6	1	1	1
1.229	3					1.231	4	4	2	3	1.232	4	4	2	2
						1.224	6	2	0	2	1.225	6	2	0	2
						1.182	5	4	1	1					

[a] A scan from 20° to 80° (2θ) using CuK_α radiation was used, and I/I_o is given as peak intensity.

[b] Four weak α-Bi_2O_3 peaks are not included.

[c] The bismuth oxide films on the glass and MgO substrates were treated in O_2 for 30 minutes at 150 ℃ at 1 Torr.

[d] ref. 16.

[e] ref. 5.

[f] Unresolved doublet due to broadening.

because the thinner 2000–3000 Å films produced eight or less reflections. Included in Table II are *d*-values obtained from a green dendritic powder collected in the vicinity of the source, and identified as the β-form. The chemical analysis of the powder showed 91.6 wt% bismuth, thus indicating that the powder is nonstoichiometric. Nearly identical powder patterns occur for β-Bi_2O_3 and β-$Bi_2O_{2.5}$ because their structures possess the same space groups along with similar cell parameters (Table I) and atom positions. The location of the bismuth atoms in both structures (*5*, *16*) is nearly identical with greater differences for the oxygen atoms. The nonstoichiometric form has two less oxygen atoms per cell forming an oxygen deficient β-Bi_2O_3. The agreement between the observed and calculated *d*-values and their intensities illustrates that the stoichiometry of the bismuth oxide films can not be determined from X-ray results alone. The above agreement combined with the chemical analysis suggests the films are nonstoichiometric, and the β-form can support an oxygen deficiency. The (200) reflection of the MgO substrate masked four weak reflections (see Table II). However, these reflections were not critical for identification. The cell parameters for the treated low rate films are listed in Table III. Little or no change is observed with respect to the length of treatment, and the values agree with those obtained by previous investigators (*4*, *5*, *16*). This agreement of the cell parameters amplifies the suggestion made with earlier mentioned X-ray results that β-Bi_2O_3 is a defect structure.

TABLE III

REFINED LATTICE PARAMETERS FOR TREATED BISMUTH OXIDE FILMS[a]

Treatment time (min)	Lattice parameters (Å)
15.0	$a = 7.753 \pm 0.003$ $c = 5.630 \pm 0.004$
30.0	$a = 7.751 \pm 0.003$ $c = 5.624 \pm 0.005$
90.0	$a = 7.753 \pm 0.003$ $c = 5.635 \pm 0.003$

[a] Copper radiation was used with the modified Debye–Scherrer technique. The films were on glass substrates. (Also, compare values with Table I.)

The presence of oxygen during thermal treatment enhanced crystallite growth. As-evaporated films treated in air did not convert to the β-form as rapidly as those treated in oxygen. The patterns of the air treated films always possessed broader peaks and lower intensities. A broad peak was noted at 28° (2θ) along with four very weeak reflections for bismuth oxide films treated in vacuum for 30 min. Further heating resulted in the formation of the α-form. All samples were scanned on the diffractrometer several times during the course of this investigation. A comparison of the patterns showed no deviations in peak positions or intensities. Prolonged thermal treatment, usually 3 or more hours, of the as-evaporated films always resulted in the formation of the α-form, whose patterns agree with those found in the literature (*12*, *13*).

The instability of Bi_2O_3 during evaporation (*21*) and the large pressure increase due to oxygen (*22*, *23*) is consistent with the formation of nonstoichiometric films. The above facts can be explained by the incongruent evaporation of Bi_2O_3. Structural disorder, the presence of impurities and deviations from stoichiometry will cause in general a spreading of the absorption edge. Impurity effects are negligible for the films used in this study. Structural disorder causes the electronic states at the band edge to tail into the band gap, and departures from stoichiometry also may introduce electronic states into the band gap directly or by induced disorder. Probe analysis showed that the bismuth content along with the Bi/O ratio increases during evaporation (*23*). The optical absorption edge broadens and shifts to lower energies by conducting consecutive evaporations or by decreasing the evaporation rate. The less disordered low rate films showed the greatest shift of their absorption edge, which is probably due to changes in stoichiometry. The Bi/O ratios are plotted against photon energy for $\alpha = 1.6 \times 10^5\ \mathrm{cm}^{-1}$ in Fig. 3. Points A through D are the calibration points. The remaining

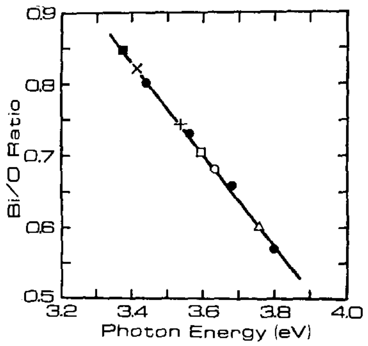

FIG. 3. Stoichiometry variations with the absorption-edge energy. ●, A, . . . , D calibration films; as-evaporated films: △, 20 Å/sec; ○, 15 Å/sec; ■, 5 Å/sec. Thermally treated films: □, 90 min; +, 30 min; ×, 15 min. The films were treated in O_2 at 150°C, 1 torr; evaporation rate, 5 Å/sec.

points are for the as-evaporated and thermally treated films.

The absorption edge for the high rate films occurs at higher energies than noted for low rate films treated in this study or for Bi_2O_3 in earlier studies (*8*). These high rate films are oxygen-rich with respect to Bi_2O_3. The compositions of the as-evaporated films determined from Fig. 3 vary from $Bi_2O_{3.5}$ (25 Å/sec) to $Bi_2O_{2.38}$ (5 Å/sec). The high rate films are oxygen-rich and amorphous, while the low rate films are microcrystalline and bismuth-rich. The absorption edge of the low rate films are microcrystalline and bismuth-rich. The absorption edge of the low rate films treated in oxygen decreases and the edge shifts to higher energies as the time of treatment increases (*24*). This information supports the suggestion that the shifts in the absorption edge are due to changes in stoichiometry. The photon energy for a low rate film treated for 15 min is 3.40 eV. This corresponds to a Bi/O ratio of 0.825 or an approximate compound formula of $Bi_2O_{2.42}$. Formulae of $Bi_2O_{2.7}$ and $Bi_2O_{2.85}$ are determined for 30 and 90 min treatments, respectively. Comparing the compositions of these treated films to the β-form further suggests a defect structure, which commonly occurs for many high temperature phases. Comparison of X-ray and stoichiometry results demonstrates that the β-form can support an oxygen-deficient structure. The formula for β-Bi_2O_3 should be written as β-$Bi_2O_{3\pm x}$, where x is the deviation from trioxide stoichiometry. On this basis, β-$Bi_2O_{2.5}$ is not an independent phase but is a nonstoichiometric β-Bi_2O_3. The deviations from the trioxide stoichiometry are reduced by thermal treatment in oxygen. These deviations varied from −0.58 to −0.15 for treated films, and from +0.5 to −0.62 for the as-evaporated films.

The formation of amorphous films at high rates can be attributed to the possible formation of defects (voids) during the coalescence of the film, and the formation of fine-sized crystallites. The existence of voids causing porosity may be the reason why higher treatment temperatures are necessary for the high rate films (*22*, *24*) and why their densities are lower (*23*). Similar defects have been suggested earlier by Thèye (*28*) for germanium films evaporated at high rates. Electron micrographs indicate that defects or voids do exist in thin amorphous films (320 Å), which are on the order of 20–50 Å. To establish the existence of these inhomogeneities in thicker films, a more detailed study is required.

The composition of the as-evaporated low rate films suggests a common vapor species. Polymeric units of $Bi_nO_n^+$, where $n = 1, \ldots, 4$, have been reported in the literature (*29*) for a Bi_2O_3 vapor heated below 900°C. The amorphous film's oxygen-rich composition may result from a more complex vapor species such as $Bi_mO_n^+$, where $m \neq n$ and $m < n$, similar to those reported for the laser-induced vaporization of Bi_2O_3 (*30*).

Conclusions

The δ- and β-form of Bi_2O_3 can be formed by the evaporation of Bi_2O_3 and the thermal treatment of bismuth oxide film, respectively. The formation of δ-Bi_2O_3 from an amorphous film demonstrates that the Bi_2O_3 melt and the as-evaporated films are structurally similar to δ-Bi_2O_3. The as-evaporated films were both disordered and nonstoichiometric. High-rate films (15–25 Å/sec) were amorphous and ranged from oxygen-rich to bismuth-rich depending on the elapsed time after the start of the evaporation. Low rate films (1–5 Å/sec) were always bismuth-rich even though their structures were more ordered. Deviation from stoichiometry results from the decomposition of Bi_2O_3 associated with its incongruent evaporation.

The formation of the β-form by thermal treatment is enhanced by the presence of an oxygen atmosphere. Treatment in oxygen also reduces the deviation from trioxide stoichiometry when the films are bismuth-rich. Comparison of the X-ray and the stoichiometry results demonstrates that the β-form can support an oxygen-deficient structure. This study suggests that β-Bi_2O_3 should be expressed as β-$Bi_2O_{3\pm x}$, where x is the deviation from the trioxide stoichiometry.

Shifts in the absorption edge may be correlated directly with the deviations from stoichiometry. The high-rate amorphous films are due to the formation of very fine-sized crystallites, and the formation of voids during the coalescence of the films. The composition of the low-rate as-evaporated films suggests common vapor species of BiO^+ and $Bi_2O_2^+$, which occur during the incongruent evaporation of Bi_2O_3.

Acknowledgments

This work was supported in part by the General Telephone and Electronics Company. The author would like to thank Dr. Richard C. Martin and Dr. Robert L. Snyder of Alfred University for their encouragement and helpful discussions throughout this investigation. Special thanks is given to Dr. J. Halford, Duke University, Durham, N.C., for supplying the calibration films and his bismuth analysis. Thanks also are given to Dr. Joe Wong, General Electric Research, and Mrs. Mildred Read, Bell Laboratories, and Dr. Robert Condrate for their helpful discussions and review of the manuscript.

References

1. L. G. Sillén, *Ark. Kemi* **12A**, 18, 1 (1937).
2. G. Gattow and H. Schröder, *Z. Anorg. Allg. Chem.* **318**, 284, 176 (1962).
3. A. A. Zav'yalova and R. M. Imamov, *Sov. Phys. Crystallogr.*, **14**, 2, 261 (1969).
4. G. Gattow and D. Schütze, *Z. Anorg. Allg. Chem.* **328**, 44 (1964).
5. A. A. Zav'yalova and R. M. Imamov, *Sov. Phys. Crystallogr.* **16**, 3, 437 (1971).
6. A. A. Zav'yalova and R. M. Imamov, *Sov. Phys. Crystallogr.* **9**, 6, 724 (1965).
7. A. A. Zav'yalova and R. M. Imamov, *Sov. Phys. Crystallogr.* **13**, 1, 37 (1968).
8. H. Gobrecht, S. Seeck, H. E. Bergt, A. Märtens, and K. Kossmann, *Phys. Status Solidi* **33**, 599 (1969).
9. M. L. Lieberman and R. C. Medrud, *J. Electrochem. Sov.* **116**, 2, 244 (1969).
10. M. G. Hapase, V. B. Tare, and A. B. Biswas, *Indian J. Pure Appl. Phys.* **5**, 9, 401 (1967).
11. L. G. Sillén, *Z. Kristallogr.* **A103**, 274 (1941).
12. G. Malmros, *Acta Chem. Scand.* **24**, 2, 384 (1970).
13. H. E. Swanson, M. C. Morris, E. H. Evans, and L. Ulmer, *Nat. Bur. Stand.* (*U.S.*), *Monogr.* 25, Sec. 3, 17 (1964).
14. E. M. Levin and R. S. Roth, *J. Res. Nat. Bur. Stand.* **68A**, 2, 189 (1964).
15. W. C. Schumb and E. S. Rittner, *J. Amer. Chem. Soc.* **65**, 1055 (1943).
16. B. Aurivillius and G. Malmros, *Trans. Roy. Inst. Technol.* (*Stockholm*, No. 291, 3 (1972).
17. A. A. Zav'yalova, R. M. Imamov, and Z. G. Pinsker, *Sov. Phys. Crystallogr.* **10**, 4, 401 (1966).
18. L. H. Gadgil and A. Goswami, *Indian J. Chem.* **8**, 431 (1970).
19. A. A. Zav'yalova and R. M. Imamov, *J. Struct. Chem. USSR* **13**, 5, 811 (1972).
20. R. J. Ackermann and R. J. Thorn, *Progr. Ceram. Sci.* **1**, 39 (1961).
21. A. Milch, *Thin Solid Films* **17**, 231 (1973).
22. J. W. Medernach, Ph.D. thesis, Alfred University, Alfred, N.Y., 1973.
23. J. Halford, Ph.D. thesis, Duke University, Durham, N.C., 1974.
24. J. W. Medernach and R. C. Martin, *J. Vac. Sci. Technol.* **12**, 1, 63 (1975).
25. J. Halford and H. Hacker, Jr., *Thin Solid Films* **4**, 265 (1969).
26. R. L. Snyder, Alfred University Research Foundation Report (1973).
27. C. A. Angell and J. Wong, *J. Chem. Phys.* **53**, 5, 2053 (1970).
28. M. L. Thèye, *Optics Commun.* **2**, 7, (1970); *Mater. Res. Bull.* **6**, 103 (1971).
29. E. K. Kazenas, D. M. Chizhikov, Yu. V. Tsvetkov, and M. V. Ol'shevskii, *Dokl. Akad. Nauk SSSR* **207**, 2, 354 (1972).
30. V. S. Ban and E. Knox, *J. Chem. Phys.* **52**, 1, 243 (1970).